Unbridged Zirconium and Titanium Metallocenes with Seven- or Eight-Saturated Fused-Ring Ligands: a Route for the Synthesis of Stereoblock Polypropene

Simona Losio,[†] Gaetano Zecchi,[†] Fabio Bertini,[‡] Maria Carmela Sacchi,*[,‡] Valerio Bertolasi,[§] and Eleonora Polo*[,∥]

Università dell'Insubria, Dipartimento di Scienze Chimiche e Ambientali, via Valleggio 11, 22100 Como, Italy, ISMAC−CNR via E. Bassini 15, 20133 Milano, Italy, Centro di Strutturistica Diffrattometrica, Dipartimento di Chimica, Università di Ferrara, via L. Borsari 46, 44100 Ferrara, Italy, and ISOF−CNR Sezione di Ferrara, via L. Borsari 46, 44100 Ferrara, Italy

Received March 22, 2005; Revised Manuscript Received June 16, 2005

ABSTRACT: Unbridged zirconocene catalysts, where a seven- or eight-membered ring fused to a cyclopentadiene is associated with a phenyl substituent in position 2 (**C_7Ph-Zr** and **C_8Ph-Zr**), were tested, under the same polymerization conditions, to produce polypropenes with microstructure, molecular properties, and thermal behavior similar to those prepared with $(IndPh)_2ZrCl_2$ (**w-Zr**), the "classical" Waymouth catalyst. Different results were obtained from the homologue titanium catalysts (**C_7Ph-Ti** and **C_8Ph-Ti**) and from the titanium benzyl derivative (**C_7Bn-Ti**), which produced quite heterogeneous materials with broad molecular weight and that can be separated into fractions spanning from completely atactic to fractions characterized by the presence of long isotactic blocks. A quite interesting behavior is observed with the zirconium benzyl derivative **C_7Bn-Zr**, which produces good yields of a polymer with narrow polydispersity, which, despite its rather high isotacticity, shows a hardly detectable melting peak and is completely ether soluble. Quite surprisingly, the same sample, after prolonged annealing, shows a narrow melting peak at low temperature (55−65 °C). This result, together with the X-ray analysis, is in favor of a quite homogeneous material, capable of giving crystallites of small size.

Introduction

In the last twenty-five years, metallocene-based catalytic systems[1] have started to find increasing industrial applications, and they now play an important role as highly active catalysts for the homo- and copolymerization of α-olefins. The scientific interest arises primarily from their single center nature and from the availability of a large variety of π-ligand structures that allow the preparation of polymers with a wide range of microstructures and properties. Metallocene-based single-site catalysts have recently become of interest also in the production of elastomeric polypropene (elPP). The first report about this type of polymer dates from 1957, when Natta[2] described the production of a rubbery polypropene and interpreted its properties in terms of a stereoblock structure consisting of alternating isotactic and atactic blocks. Later on, Collette and co-workers[3] developed Ti and Zr alkyls supported on alumina that provided significant amounts of elPP, allowing a more detailed study of its properties. More recently, other authors[4] have synthesized stereorigid unsymmetrical *ansa*-metallocenes that produced elPP of narrow molecular-weight distribution under a variety of conditions. But the real breakthrough was the discovery by Waymouth and Coates[5] that elPP can be produced using a nonbridged metallocene, bis(2-phenylindenyl)zirconium dichloride. Indeed, through a rational choice of the polymerization conditions,[6] this catalyst can produce polymers containing, besides a variable amount of an essentially atactic fraction, a minor fraction of prevailingly isotactic polypropene. In this fraction, a melting transition was detected, and so demonstrating that the isotactic sequences were long enough to be capable of crystallizing. To account for these data, the authors introduced the concept of "fluxional" catalysts that describes the behavior of unbridged metallocenes able to interconvert between chiral and achiral rotational isomers on the time scale of the polymerization reactions. This intuition led to an extensive exploration about the sterical requirements and the reaction conditions able to control/improve the performance of the reference catalyst. As long as the number of catalytic systems studied increased, their behavior appeared to be more complicated than it seemed at the beginning. The early mechanism was later questioned by several authors[7] and reformulated by Waymouth himself.[8] Indeed, a 2-substituted *meso*-bis(indenyl)ZrX_2 metallocene rotamer, considered responsible for the atactic segment, has never been detected in solution and its equilibration with the *rac*-conformer has never been experimentally demonstrated, as pointed out in the thorough work by Erker.[9] Despite the number of papers appearing in the last few years, a complete understanding of the behavior of this type of catalyst is still controversial[7−10] and prevents a precise prediction of the catalyst stereoselectivity for a given ligand environment. What seems quite established is that there are substantially two kinds of factors that can increase the life of catalytic species capable of producing long isotactic blocks: the steric hindrance of the ligands (bulky substituents in fixed positions can give a quite high isotactity) and the type of cocatalyst[11] (e.g., compared to MAO, some perfluoroarylborate anions can produce

* Authors to whom correspondence should be addressed. E-mail: tr3@unife.it (E.P.); sacchi@ismac.cnr.it (M.C.S.). Fax: +39 0532240709 (E.P.); +39 0270636400 (M.C.S.).
[†] Università dell'Insubria.
[‡] ISMAC−CNR.
[§] Università di Ferrara.
[∥] ISOF−CNR.

10.1021/ma050599t CCC: $30.25
Published on Web 07/20/2005

an increase of tacticity even of the 20%). The most effective structural variations have been proposed mainly by Waymouth and co-workers.[6] Although there are some exceptions, the replacement of the basic indenyl ligand by a saturated system or by a bulkier aromatic ligand usually produces a significant loss of capacity of the catalyst to give isotactic blocks. The presence and the substitution pattern of an aryl substituent in position 2 seems also to play an essential role in the polymerization outcome. There is one only case in which a substitution in this position significantly improves the catalyst performance, i.e., when the substituent is a benzyl.[12]

A few years ago, we decided to enter such a fascinating field by investigating a new family of unbridged catalysts based on a bicyclic ligand with a saturated ring of different sizes (six, seven, and eight carbon atoms) fused to a cyclopentadiene and bearing different substituents in position 2. Our aim was to investigate the possibility to observe a "fluxional behavior" and to obtain elPP, even in the absence of the aromatic ring, by introducing the conformational flexibility of the saturated ring as a new parameter. We studied several sets of complexes, concentrating our attention not only on the substituents on the indenyl ligand, but also on the role played by the saturated ring condensed to the cyclopentadienyl moiety.[13] Up to then, the lack of a synthetic strategy able to allow systematic variations with respect to the basic catalyst structure, had prevented investigations of this kind.

After a systematic investigation on several 2-substituted bicyclic zirconocenes, we have successively investigated the effect of the change from zirconium to titanium on the most promising structures.[14] Because the titanium center allows a closer interaction between the two bent cyclopentadienyl moieties, the effect of the substituents should have exerted a stronger influence on the interconversion speed between aspecific and isospecific isomers, thus favoring the formation of longer isotactic blocks. The well-known easy decomposition[4d−e,10b,15] of indenyl titanium complexes during polymerization had so far prevented their study in this field. The saturated ring showed an inference of a higher stability to these complexes, thus allowing, for the first time, a full characterization of a polypropene sample obtained through titanium-based catalysts. In the present paper, we report a complete picture of the most promising results obtained, both with the zirconium and the titanium catalysts synthesized, under more proper polymerization conditions (higher propene pressure). The replacement of the phenyl group in position 2 for a benzyl, with the target of improving the catalysts' stereocontrol and productivity, was also investigated.

Results and Discussion

Metallocene Synthesis and Characterization. The phenyl-substituted complexes (**C_7Ph-Zr**, **C_8Ph-Zr**, **C_7Ph-Ti**, **C_8Ph-Ti**, **w-Zr**, and **w-Ti**) (Scheme 1) were synthesized as described previously.[13,15,16]

The benzyl complexes (**C_7Bn-Zr** and **C_7Bn-Ti**) were prepared according to Scheme 2, starting from the enone (**1**), the same intermediate used for the synthesis of the phenyl derivatives.[17] Reaction of the enone (**1**) with benzylmagnesium chloride, followed by quenching with diluted HCl, gave the diene (**2**), which was treated with a slight excess of *n*-butyllithium to give the corresponding lithium salt (**3**).

Scheme 1

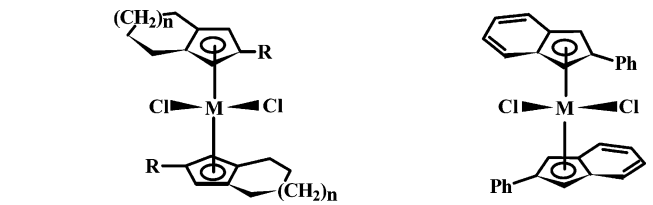

M= Zr R= -Ph; n= 2 (**C_7Ph-Zr**); 3 (**C_8Ph-Zr**)
R= $-CH_2Ph$; n= 2 (**C_7Bn-Zr**)
M= Ti (**w-Ti**)
M= Zr (**w-Zr**)
M= Ti, R= -Ph; n= 2 (**C_7Ph-Ti**); 3 (**C_8Ph-Ti**)
R= $-CH_2Ph$; n= 2 (**C_7Bn-Ti**)

Scheme 2

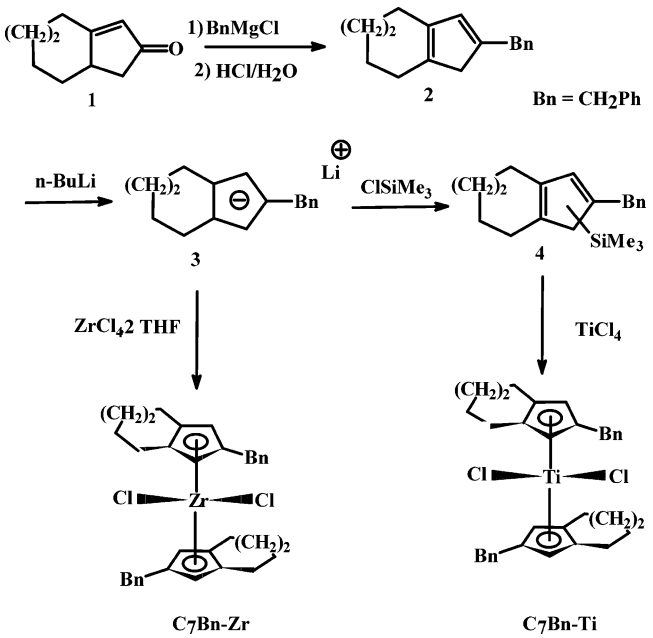

The zirconium derivative (**C_7Bn-Zr**) was prepared by direct reaction with $ZrCl_4$·2THF, while we found that, as in the case of the corresponding phenyl derivatives, the synthesis by direct reaction of the lithium salt (**3**) with $TiCl_4$ in THF (or with $TiCl_3$ followed by oxidation with $PbCl_2$) gave poor yields of an extremely difficult-to-purify complex. This problem seems to be due to the easy reduction/decomposition of the Ti complexes either by visible light in solution (in particular in THF) or by residual traces of alkyllithiums from the previous deprotonation step. This problem was overcome by converting the lithium salt (**3**) into its corresponding air-stable trimethylsilyl derivative (**4**) and by carrying the metalation reaction in CH_2Cl_2, taking care of shading the reaction vessel from light. The complex was easily collected by elimination under vacuum of the solvent and of the $ClSiMe_3$ produced in the reaction, followed by washing with petroleum ether.

In the case of **C_7Bn-Zr**, proper crystals for X-ray diffraction were collected (ORTEP[18] view of the compound is shown in Figure 1).

The complex displays a distorted tetrahedral geometry, with the tetrahedron defined by the two chlorine atoms and the centroids of two η^5-cyclopentadienyl rings of 2-benzyl-4,5,6,7,8-hexahydroazulenyl ligands. The complex lies on a crystallographic 2-fold axis passing through the Zr1 atom; the cyclopentadienyl rings are eclipsed. The seven-membered rings of the hexahydroazulenyl ligands lie on opposite sides, as well as the

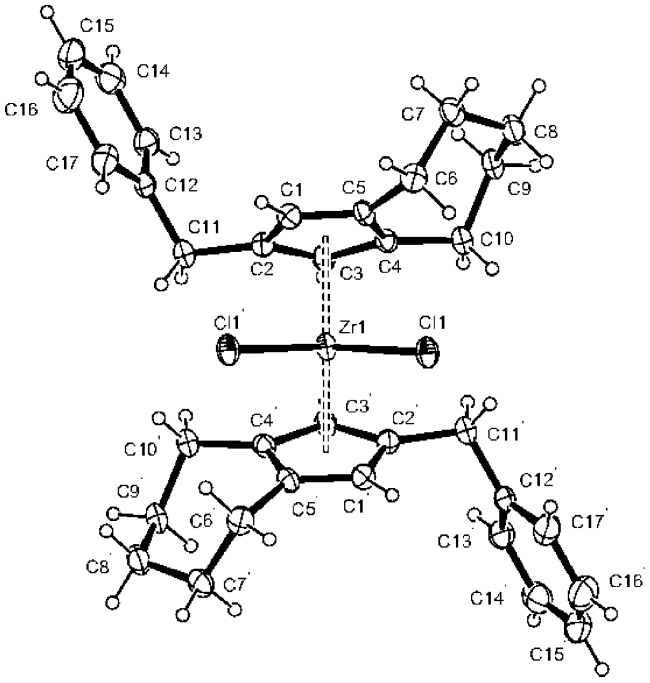

Figure 1. ORTEP view of **C_7Bn-Zr** displaying the thermal ellipsoids at 30% probability.

Table 1. Selected Bond Distances (Å) and Angles (deg) for C_7Bn-Zr

Zr1−Cl1	2.446(2)	Zr1−Cp1	2.228(6)
Zr1−C1	2.529(6)	C1−C2	1.410(10)
Zr1−C2	2.480(7)	C1−C5	1.400(8)
Zr1−C3	2.496(7)	C2−C3	1.418(9)
Zr1−C4	2.554(6)	C3−C4	1.411(8)
Zr1−C5	2.593(6)	C4−C5	1.412(10)
Cl1−Zr1−Cl1′	98.8(1)	Cp−Zr1−Cp′	133.2(2)
Cl1−Zr1−Cp[a]	105.6(2)	C1−C5∧C1′−C5′[b]	50.9(2)

[a] Cp = Centroid of the cyclopentadienyl ring: C1−C5. [b] Dihedral angle between the cyclopentadienyl rings.

benzyl groups. The distances and angles around the Zr1 atom (Table 1) are similar to those found in other $(RCp)_2ZrCl_2$ unbridged metallocenes with bulky R groups[19] and in unbridged $(Ind)_2ZrCl_2$ indenyl derivatives,[5,20] but both the Cl−Zr−Cl and Cp−Zr−Cp angles are a bit larger than those reported for other "fluxional catalysts", suggesting the presence of a more "open" catalytic center.

Zirconium Phenyl Catalysts. In a previous work,[13] we carried out a preliminary screening of three series of complexes with a six-, seven- or eight-membered saturated ring, respectively, and differently substituted (−H, $-CH_3$, −Ph) in position 2, at three temperatures (30, 0, and −20 °C), at 1 atm propene pressure.

In the present paper, the two most promising catalysts, where a seven- or an eight-membered ring is associated with a phenyl substituent in position 2 (**C_7Ph-Zr** and **C_8Ph-Zr**), were tested in propene polymerization at two different temperatures (0 and −15 °C) and at a propene pressure of 2.4 atm. Table 2 shows the polymerization data of the samples, along with the microstructural, molecular, and thermal properties. Because the oscillating behavior is extremely sensitive to the polymerization conditions, we have taken as reference the "classical" Waymouth catalyst (**w-Zr**), synthesized in our labs, and compared step-by-step the results obtained with the new catalysts with those given by **w-Zr** under the same polymerization conditions.

The patterns of the ^{13}C NMR spectra of the samples produced with the new catalysts and of those obtained with **w-Zr** are quite similar. It is worth noticing that decreasing temperature from 0 to −15 °C is not beneficial for **w-Zr**. In principle, a decrease in temperature should slow both the propagation speed and the rate of interconversion of isospecific and aspecific states. It is likely that the equilibrium between the two effects in **w-Zr** at −15 °C is shifted in favor of the first one, with a consequent lowering of the length of the isotactic blocks. In particular, the spectrum of the polymer prepared with **C_7Ph-Zr** at −15 °C is almost identical to that obtained with **w-Zr** at 0 °C (Figure 2). This is a further evidence of the fact that very subtle structural differences are crucial for the oscillating behavior of the catalyst.

The activities, the isotactic pentads content, the thermal behavior, and the average length of isotactic sequences N_{iso} ($N_{iso} = 4 + 2\ [mmmm]/[mmmr]$)[21] are comparable.

The appearance of broad melting transitions spanning from 90 to 150 °C in the moderately isotactic samples from **C_7Ph-Zr** and **C_8Ph-Zr**, the same phenomenon observed in the sample prepared with **w-Zr**, allows us to hypothesize that **C_7Ph-Zr** and **C_8Ph-Zr** can also produce isotactic blocks. The molecular weights of polypropenes obtained with the zirconium catalysts **C_7Ph-Zr** and **C_8Ph-Zr** are of the same order of magnitude as those obtained with **w-Zr**, but the polydispersity is about 2 (typical of single-site catalysts), while it is higher (3−4) for the reference catalyst.

A fractionation with boiling diethyl ether was carried on all the samples. All the samples, including those from **w-Zr**, were almost completely soluble or separable into a boiling diethyl ether soluble and an insoluble fraction of almost identical tacticity (in these cases, the molecular weight plays certainly a significant role in the sample solubility). This behavior, that differs from most literature data,[22] is supposed to be due to the fact that, under our polymerization conditions, it is not possible to obtain isotactic segments long enough to give ether insoluble fractions.

Table 2. Results of Propene Polymerization with Zr Catalysts at 2.4 Atm[a]

entry	catalyst	T_{pol} (°C)	activity (Kg_{PP}/mol_{Zr}*h)	[*mmmm*][b]	N_{iso}[c]	T_m range[d] (°C)	ΔH_m[d] (J/g)	MW*10^{-3} [e]	PDI[e]
1	w-Zr	0	469.9	15.9	6.2	120−150	0.3	297	4.1
2	w-Zr	−15	193.9	11.9	5.6	90−105	<0.1	144	3.2
3	C_7Ph-Zr	0	96.2	14.0	5.6	90−110	<0.1	265	2.1
4	C_7Ph-Zr	−15	346.6	17.4	5.9	125−150	0.4	224	2.1
5	C_8Ph-Zr	0	372.7	13.6	5.5	100−140	0.2	125	1.8
6	C_8Ph-Zr	−15	251.9	16.3	5.7	110−150	0.3	157	2.5

[a] Reaction conditions. Toluene: 100 mL, [Mt] = 10×10^{-5} mol/L, [MAO]/[Mt] = 1000, t_{rxn} = 1 h. [b] Isotactic pentad contents by ^{13}C NMR. [c] Average length of isotactic blocks estimated by ^{13}C NMR. [d] Determined by differential scanning calorimetry (DSC) on second heating scan. [e] Molecular weight and polydispersity determined by SEC.

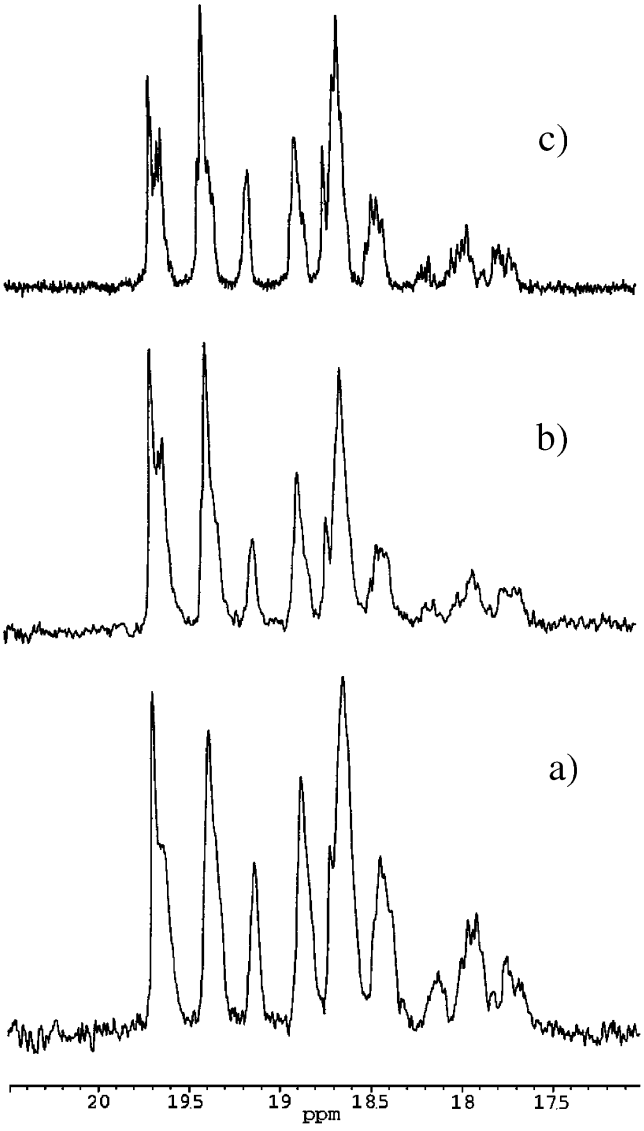

Figure 2. ^{13}C NMR spectra of polypropenes prepared with **w-Zr** (a) (Table 2, entry 1), **C_7Ph-Zr** (b) (Table 2, entry 4), and **C_8Ph-Zr** (c) (Table 2, entry 6).

Titanium Phenyl Catalysts. In Table 3 are reported the polymerization, microstructural, and molecular data, together with the thermal behavior of the samples obtained with the homologous titanium metallocenes (**C_7Ph-Ti**, **C_8Ph-Ti**, and **w-Ti**). Polymerizations were carried out at the constant propene pressure of 2.4 atm at 0 and −15 °C.

As to the activities (Table 3), the acceptable polymer yields (although lower than from their zirconium homologues) obtained with **C_7Ph-Ti** and with **C_8Ph-Ti** at 0 °C, despite the well-known low stability of titanium-based metallocenes, are a quite remarkable result. On the contrary, **w-Ti**, likely due to the unsaturated ring, is a less-effective catalyst.

Only in entry 6 of Table 3 (sample from **C_8Ph-Ti** at low temperature) can we appreciate the expected increase in isotacticity (from 16.3% with **C_8Ph-Zr** to 21.9% with **C_8Ph-Ti**). With the other catalysts, in particular, for the more productive experiments, the isotacticity is lower than that obtained with the corresponding zirconocenes. Surprisingly enough, even when the isotactic pentad content is lower (see entry 1 and 3, Table 3), the average length of the isotactic blocks (N_{iso}) is almost equal or even slightly higher than that obtained with the zirconium homologues. In fact, in the methyl region of the spectra of Figure 3, it is possible to detect in all samples the presence of the narrow signal of the [*mmmmmm*] heptad at 19.67 ppm.

Independently of the isotactic pentad content [*mmmm*], in accordance with the N_{iso} values, the melting peaks observed in the DSC spectra of polypropenes generated with titanium catalysts are more evident than with the zirconium homologues. The enthalpies of fusion are sensibly increased, and the melting peaks are shifted toward higher temperatures (115−155 °C). It is worth observing that, despite the remarkable amount of the syndiotactic [*rr*] centered pentads from 17.8 to 18.2 ppm (Figure 3), only isotactic crystallinity is observed. The molecular weights are in general similar to those of the polymers obtained with the zirconium homologues, while the molecular-weight distributions are quite a bit wider, indicating a more heterogeneous material. Such heterogeneity is also evidenced by the fact that, unlike their zirconium homologues, all samples from titanium could be separated into an ether-soluble (ES) fraction with low tacticity and an ether-insoluble (EI) fraction with higher tacticity, where the calculated average length of isotactic sequences spans from 8.1 to 11.7 ppm (Table 4). The regioirregularities detected in the fractions are directly proportional to the percents of stereoirregular sequences. This means that they belong to irregular segments, indicating that the regioirregular insertions mainly occur in the absence of any steric control of the active center. In Figure 4, the spectra of the ether-soluble (ES) and ether-insoluble (EI) fractions of the sample prepared with **C_8Ph-Ti** are compared with that of the raw polymer. The two fractions show different thermal behavior (Figure 5): the ES fraction does not exhibit any thermal transition under these experimental conditions, while the EI fraction shows a melting transition centered at 148 °C, with an enthalpy of fusion of 9.3 J/g.

Ti and Zr Benzyl Derivatives. Because the substitution of the phenyl in position 2 for a benzyl group was reported to sensibly enhance the isotacticity of **w-Zr**,[12] we have also studied the zirconium and titanium benzyl

Table 3. Results of Propene Polymerization with Ti Catalysts at 2.4 Atm[a]

entry	catalyst	T_{pol} (°C)	activity (Kg_{PP}/mol_{Ti}*h)	[*mmmm*][b]	N_{iso}[c]	T_m range[d] (°C)	ΔH_m[d] (J/g)	MW*10^{-3}[e]	PDI[e]
1	w-Ti	0	44.4	6.7	6.1	125−155	0.3	87	4.4
2	w-Ti	−15	20.1	14.2	6.7	120−155	1.0	150	4.0
3	C_7Ph-Ti	0	141.5	5.5	5.8	120−155	0.5	290	5.8
4	C_7Ph-Ti	−15	145.5	7.9	6.2	120−155	1.2	234	6.5
5	C_8Ph-Ti	0	82.4	9.9	6.5	115−155	0.9	276	4.8
6	C_8Ph-Ti	−15	36.5	21.9	8.3	115−155	3.6	215	3.8

[a] Reaction conditions. Toluene: 100 mL, [Mt] = 10 × 10^{-5} mol/L, [MAO]/[Mt] = 1000, t_{rxn}= 1 h. [b] Isotactic pentad contents by ^{13}C NMR. [c] Average length of isotactic blocks estimated by ^{13}C NMR. [d] Determined by differential scanning calorimetry (DSC) on second heating scan. [e] Molecular weight and polydispersity determined by SEC.

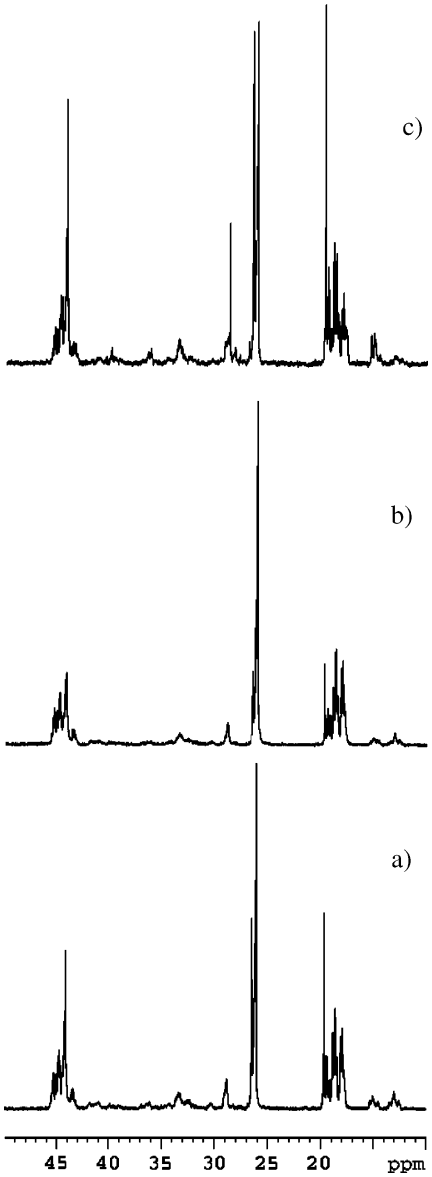

Figure 3. ^{13}C NMR spectra of polypropenes prepared with **w-Ti** (a) (Table 3, entry 2), **C_7Ph-Ti** (b) (Table 3, entry 4), and **C_8Ph-Ti** (c) (Table 3, entry 6).

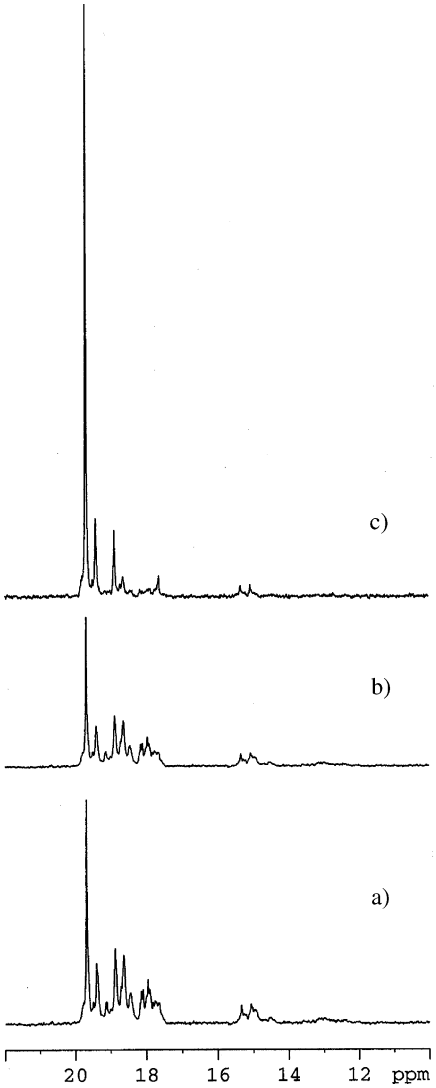

Figure 4. Expansion of the ^{13}C NMR methyl region of raw polymer (a), ether-soluble (b), and ether-insoluble (c) fractions of the sample prepared with **C_8Ph-Ti** (Table 3, entry 6).

derivatives (**C_7Bn-Zr** and **C_7Bn-Ti**) of the seven-membered complexes. In Table 5 are reported the polymerization data and the microstructural, molecular, and thermal properties of the polypropenes obtained. Also, in this case, the activity of the zirconium catalyst is significantly higher than that of its titanium homologue. As expected, the NMR analysis (Figure 6) shows, in both cases, a remarkable increase of isotacticity compared to that of the corresponding phenyl derivatives.

The polymers produced from **C_7Bn-Ti** are quite similar to those obtained from **C_7Ph-Ti**. They also have a broad molecular-weight distribution and show an evident melting peak centered at about 140 °C. Their heterogeneous nature is demonstrated by the fact that they can be separated into fractions of increasing isotacticity. Figure 7 shows the methyl region of the

Table 4. Polymer Fractionation Data

entry	catalyst	wt %	[*mmmm*][a]	N_{iso}[b]	regioirregularity[c] (%)	T_m range[d] (°C)	ΔH_m[d] (J/g)	MW*10^{-3}[e]	PDI[e]
2	w-Ti	100	14.2	6.7	6.6	120−155	1.0	150	4.0
ES		73	3.7	5.1	9.4		amorphous	114	2.8
EI		27	44.8	10.0	4.9	125−155	3.2	198	3.2
4	C_7 Ph-Ti	100	7.9	6.2	6.6	120−155	1.2	234	6.5
ES		48	3.4	5.0	7.4		amorphous	130	2.4
EI		52	18.4	8.1	5.5	120−155	2.1	293	3.3
6	C_8 Ph-Ti	100	21.9	8.3	7.4	115−155	3.6	215	3.8
ES		60	14.5	6.3	9.8		amorphous	178	2.5
EI		40	54.8	11.7	3.3	115−155	9.3	260	3.1

[a] Isotactic pentad content determined by ^{13}C NMR. [b] Average length of isotactic blocks estimated by ^{13}C NMR. [c] Percent of regioirregular insertions from ^{13}C NMR (spectral region from 12.5 to 15.5 ppm). [d] Determined by differential scanning calorimetry (DSC) on second endotherm scan. [e] Molecular weight and polydispersity determined by SEC

Table 5. Results of Propene Polymerization with Benzyl Derivatives at 2.4 Atm[a]

entry	catalyst	T_{pol} (°C)	activity (Kg_{PP}/mol_{Mt}*h)	[mmmm][b]	N_{iso}[c]	T_m range[d] (°C)	ΔH_m[d] (J/g)	MW*10^{-3} [e]	PDI[e]
1	C_7Bn-Zr	0	188.2	24.2	6.6	105−140	0.1	35	1.9
2	C_7Bn-Zr	−15	339.2	35.0	7.8	90−125	0.2	108	2.1
3	C_7Bn-Ti	0	30.0	20.5	7.8	80−155	1.8	191	7.1
4	C_7Bn-Ti	−15	4.6	25.8	7.5	115−155	1.2	nd[f]	nd[f]

[a] Reaction conditions. Toluene: 100 mL, [Mt] = 10 × 10^{-5} mol/L, [MAO]/[Mt] = 1000, t_{rxn}= 1 h. [b] Isotactic pentad contents by ^{13}C NMR. [c] Average length of isotactic blocks estimated by ^{13}C NMR. [d] Determined by differential scanning calorimetry (DSC) on second heating scan. [e] Molecular weight and polydispersity determined by SEC. [f] Not detected.

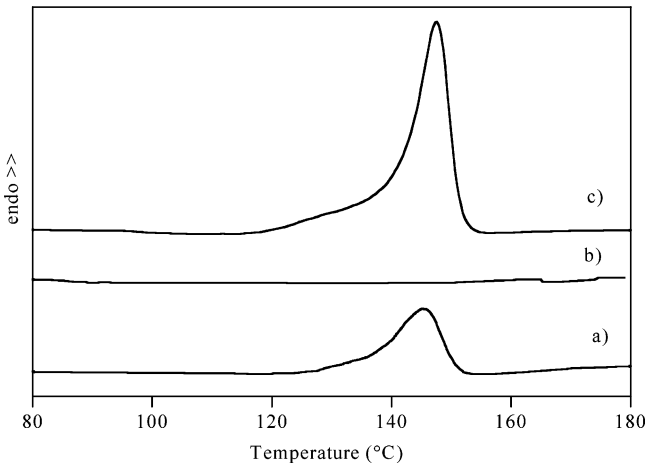

Figure 5. DSC curves of raw polymer (a), ether-soluble (b), and ether-insoluble (c) fractions of sample prepared with **C_8Ph-Ti** (Table 3, entry 6).

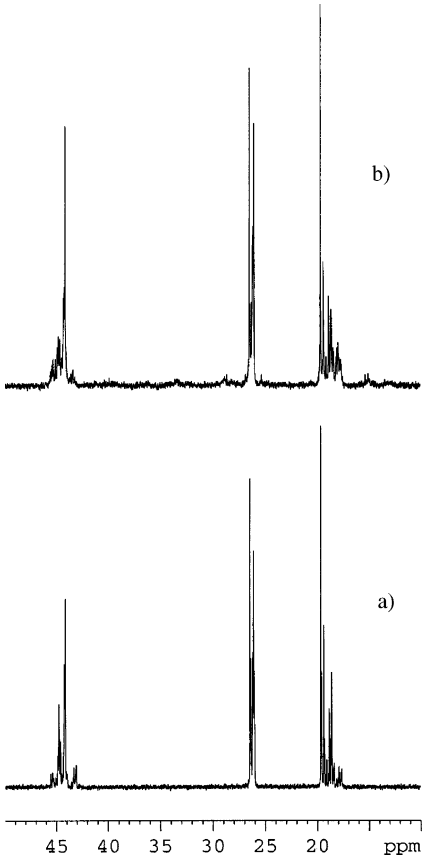

Figure 6. ^{13}C NMR spectra of polypropenes prepared with **C_7Bn-Zr** (Table 5, entry 2) and **C_7Bn-Ti** (Table 5, entry 4).

spectra of the ether-soluble (65 wt %, [*mmmm*] = 11.6, N_{iso} = 5.9), hexane-soluble (25 wt %, [*mmmm*] = 16.1, N_{iso} = 6.8), and hexane-insoluble (10 wt %, [*mmmm*] = 56.1, N_{iso} = 11.5) fractions of the sample prepared at 0 °C, while in Figure 8 are shown the thermal behavior of the raw polymer and of its fractions.

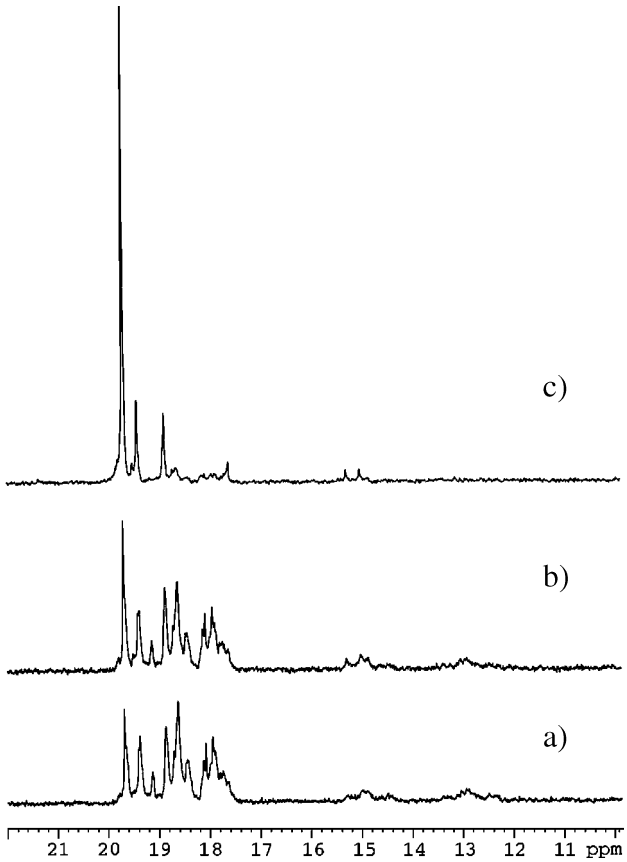

Figure 7. Expansion of the ^{13}C NMR methyl region of ether-soluble (a), hexane-soluble (b), and hexane-insoluble (c) fractions of sample prepared with **C_7Bn-Ti** (Table 5, entry 3).

The ether-soluble fraction, though not completely atactic, behaves like a completely amorphous polypropene in this experimental conditions. In the other fractions, the melting temperature and the enthalpy of fusion increase with the degree of isotacticity. The hexane-soluble fraction exhibits a small melting transition ranging from 80 to 100 °C, with an enthalpy of fusion of 0.4 J/g. A more evident endothermic event spanning from 80 to 150 °C (ΔH_m= 15.8 J/g) characterizes the DSC scan of the hexane-insoluble fraction. The degree of crystallinity, obtained by dividing the experimental heat of fusion by the enthalpy of fusion of 100% crystalline polypropene (209 J/g), is found to be approximately 8%. The wide-angle X-ray diffraction (WAXD) spectrum of the hexane-insoluble fraction (Figure 9) shows the peaks at 2θ = 14.1°, 16.8°, 18.6°, 21.2°, and 21.7°, typical of the α modification of isotactic polypropene. A crystallinity value of 12%, calculated by WAXD, is in good agreement with the value estimated by DSC analysis.

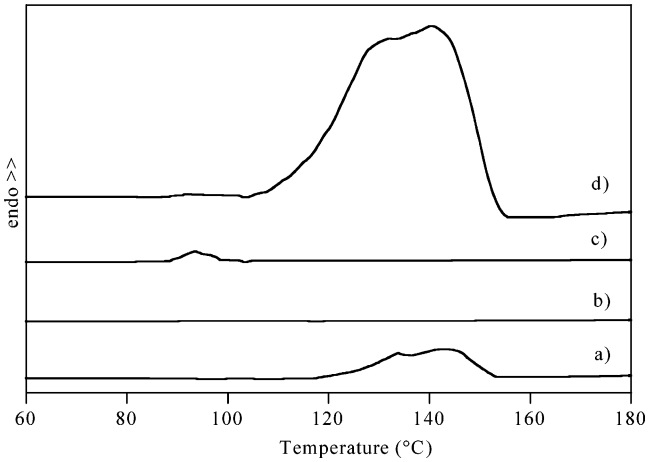

Figure 8. DSC curves of raw polymer (a), ether-soluble (b), hexane-soluble (c), and hexane-insoluble (d) fractions of sample prepared with **C_7Bn-Ti** (Table 5, entry 3).

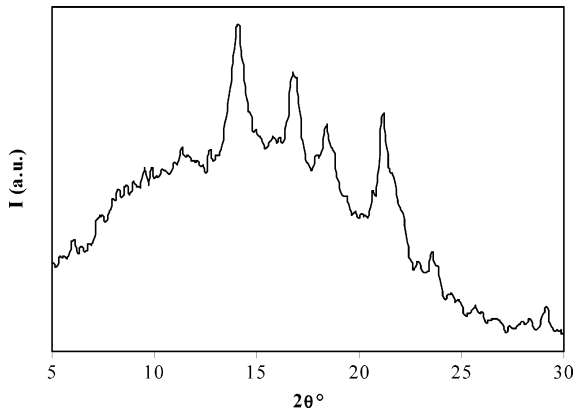

Figure 9. X-ray diffraction spectrum of hexane-insoluble fraction of sample prepared with **C_7Bn-Ti** (Table 5, entry 3).

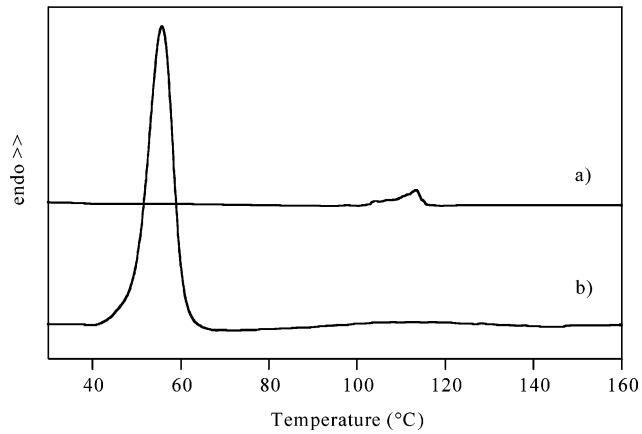

Figure 10. DSC endotherm scans of sample prepared with **C_7Bn-Zr** (a) (Table 5, entry 2) and annealed entry 2 (b).

Despite the high isotacticity, the samples obtained with **C_7Bn-Zr**, are rather surprisingly completely ether soluble. Moreover, they show a hardly detectable endothermic event in the DSC thermal analysis (Table 5). However, a different thermal behavior is observed by annealing the samples at 20 °C for prolonged periods (5−30 days). Indeed, the annealing process leads to relevant and rather narrow melting peaks at 55−65 °C. Figure 10 compares the DSC thermal profiles of entry 2 (from **C_7Bn-Zr** at −15 °C) and annealed entry 2; the annealed polymer shows an endothermic event centered at 58 °C with an enthalpy of fusion of 7.9 J/g.

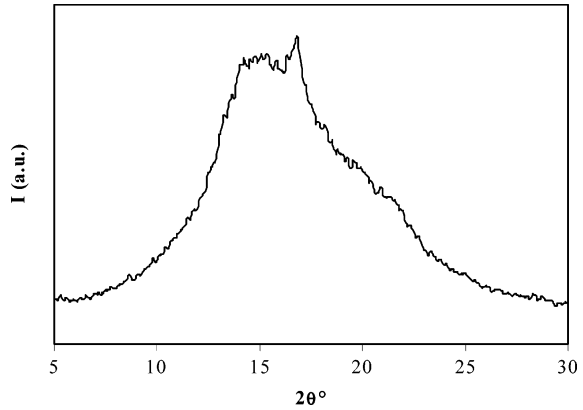

Figure 11. X-ray diffraction spectrum of annealed sample prepared with **C_7Bn-Zr** (Table 5, entry 2).

The transition is probably due to the melting of crystalline entities of small sizes and low degree of perfection. Such a hypothesis is supported by the WAXD profile (Figure 11) that confirms the presence of small crystallinity in the annealed sample.

On the contrary, the same annealing treatment does not affect the thermal behavior of the samples obtained with all the other zirconium catalysts studied. The above results indicate that the polypropene produced with **C_7Bn-Zr** is significantly different from that obtained with all the other zirconium catalysts, including **w-Zr**. In fact, samples obtained with **w-Zr** with similar isotacticity (about 30%) are reported[22] to be separable into different fractions spanning from atactic to highly isotactic. This is an indication of a wide distribution of isotactic sequences lengths. On the contrary, the complete ether solubility, the lower melting point, the narrow melting peak, and the polydispersity value (about 2), typical of a single-site catalyst, of the polypropenes from **C_7Bn-Zr** suggest the presence of shorter and more homogeneous isotactic block lengths, in accordance with its more "open" catalytic center.

Conclusion

Unbridged zirconocene catalysts, where a seven- or eight-membered ring fused to a cyclopentadiene is associated with a phenyl substituent in position 2 (**C_7Ph-Zr** and **C_8Ph-Zr**), were tested, under the polymerization conditions used, to produce polypropenes with microstructure, molecular properties, and thermal behavior similar to those prepared with $(IndPh)_2ZrCl_2$ (**w-Zr**), the "classical" Waymouth catalyst.

The results obtained show that it is possible, in principle, to observe a "fluxional behavior", and to obtain stereoblock PP, even by replacing the basic indenyl structure with a slightly flexible saturated ring. This structural feature sensibly increases the stability of the complexes, thus making possible investigation of the effect on the oscillating catalyst behavior of switching from zirconium to titanium as the metal center. The polymers obtained from the titanium catalysts (**C_7Ph-Ti** and **C_8Ph-Ti**) were rather different from those obtained from their zirconium homologues (**C_7Ph-Zr** and **C_8Ph-Zr**). Indeed, independently of the percent of total isotacticity (lower in several cases), longer isotactic blocks are undoubtedly formed with titanium catalysts, as clearly shown by more evident melting peaks. The fractionation data, along with the broad molecular-weight distribution, are in favor of quite heterogeneous materials.

Polypropenes obtained with the titanium benzyl derivative (**C_7Bn-Ti**) show almost the same characteristics of all the other samples of the series obtained with titanium catalysts. On the contrary, a quite different behavior is observed with the zirconium benzyl derivative **C_7Bn-Zr**. It produces indeed good yields of a polymer which, despite the rather high isotacticity, is completely ether soluble, has a narrow polydispersity, and, after prolonged annealing, shows a narrow melting peak at low temperature (55−65 °C). All these characteristics are in favor of a quite homogeneous material, with a relatively narrow distribution of isotactic sequence lengths, capable of giving crystallites of small sizes, which deserve a more targeted study.

Experimental Section

General Remarks. Manipulations of air- and/or moisture-sensitive materials were carried out under inert atmosphere using a dual vacuum/argon line and standard Schlenk techniques. Solvents for synthesis and NMR characterization were thoroughly dehydrated and deoxygenated under nitrogen by refluxing over a suitable drying agent (pentane, petroleum ether, diethyl ether, toluene, and THF over K; C_6D_5N over KOH; CH_2Cl_2 and $CDCl_3$ over CaH_2), followed by distillation and storage under argon in Young's ampules. Solvents and solutions were transferred, using a positive pressure of argon, through stainless steel *cannulae* (diameter 0.5−2.0 mm), and mixtures were filtered in a similar way using modified *cannulae* that could be fitted with glass-fiber filter disks (Whatman GFC).

Unless otherwise specified, all reagents were purchased from commercial suppliers (Aldrich and Fluka) and used without further purification. Zirconium(IV) chloride−tetrahydrofuran complex was prepared from $ZrCl_4$ (Strem) according to literature procedure.[23] 4,5,6,7,8,8a-Hexahydroazulen-2(1*H*)-one (**1**) was synthesized from cycloheptanone, as previously reported.[17]

Reaction courses and product mixtures were routinely monitored by thin-layer chromatography (TLC) on silica gel precoated F_{254} plates.

^{1}H (200.13 MHz) and ^{13}C (50.32 MHz) NMR spectra were recorded at room temperature with a Bruker AC200 spectrometer. Spectra were referenced internally using the residual protio solvent resonance relative to tetramethylsilane ($\delta = 0$). Elemental analyses were performed using a Carlo Erba 1106 elemental analysis apparatus.

2-Benzyl-4,5,6,7,8-hexahydroazulene (2). 10 mmol of the enone (**1**) were dissolved in anhyd diethyl ether (20 mL) and cooled to 0 °C under argon. Benzylmagnesium chloride (1.2 equiv) was added dropwise, and the resulting cloudy yellow mixture was stirred at 0 °C until the TLC (diethyl ether/petroleum ether 1:1) showed traces of the starting material (about 1 h). The reaction mixture was then quenched with cold diluted HCl solution, and the separated aqueous phase was washed several times with diethyl ether. The collected organic fractions were dried over anhyd $MgSO_4$. After filtration, the solvent was removed under reduced pressure to leave a yellow oil. A passage through a short column ($h = 5$ cm; Ø = 3 cm) of silica gel 60 (230−400 mesh ASTM) of a petroleum ether solution of the diene (**2**), a mixture of three isomers, was enough for a quick purification. The resulting yellow oil (solid at −15 °C) was obtained in a 56% yield over two steps (average yield per step 75%).

Lithium 2-benzyl-4,5,6,7,8-hexahydroazulenyl (4). The diene (**2**) (8.80 mmol) was transferred into a Schlenk flask, degassed, dissolved in anhyd petroleum ether (20 mL), and cooled to 0 °C. *n*-Butyllithium (2.5 M solution in hexanes, 12.5 mmol) was added dropwise, the solution was stirred at 0 °C for 30 min, then allowed to reach room temperature and stirred overnight. The lithium salt (**3**) separated from the solution as a dusty solid, which was filtered via a *cannula* and washed twice with petroleum ether. The residual solvent was pumped off, leaving the lithium salt (**3**) as a pale-yellow pyrophoric powder. Yield from (**1**): 30% over three steps (average yield per step: 66%). ^{1}H NMR (C_6D_5N): δ 1.83 (br s, 6H, C-CH_2-CH_2−), 2.86 (br s, 4H, −C-CH_2-CH_2−), 4.10 (s, 2H, Cp-CH_2-Ar), 5.84 (s, 2H, Cp*H*), 7.05−7.40 (m, 4H, −Ar*H*), 7.40−7.50 (m, 4H, −Ar*H*). ^{13}C NMR (C_6D_5N): δ 32.2 [−*C*H$_2$−], 33.0 [−*C*H$_2$−], 34.8 [−*C*H$_2$−], 38.1 [C-*C*H$_2$-Ar], 105.0 [−*C*H Cp], 113.2 [C$_q$, −CH_2-*C*-Cp], 119.2 [C$_q$, *C*-CH_2-Ar], 125.3 [−p*C*H-Ar], 128.5 [−m*C*H-Ar], 129.8 [−o*C*H-Ar], 147.4 [C$_q$, −CH_2-*C*-Ar].

Bis[η^5-(2-benzyl-4,5,6,7,8-hexahydroazulenyl)]zirconium Dichloride (C_7Bn-Zr). A solution of $ZrCl_4$·2THF (4.5 mmol) in THF (15 mL) was added dropwise to 9.6 mmol of the lithium salt (**3**) dissolved in anhyd THF (20 mL). The reaction mixture was stirred overnight. The solvent was removed under vacuum, and the residue was extracted with toluene, filtered, concentrated, and layered with pentane. A dusty white-yellow solid precipitated and was isolated by filtration, washing with pentane, and evaporation of the residual solvent under high vacuum. Crystals suitable for X-ray diffraction were obtained by dissolving the solid in CH_2Cl_2, and by alternating cycles of slow evaporation of the solvent and freezing at −15 °C. Yield 70%. ^{1}H NMR ($CDCl_3$): δ 1.05−2.1 (m, 12H, C-CH_2-CH_2−), 2.2−2.9 (m, 8H, −C-CH_2-CH_2−), 3.75 (s, 4H, Cp-CH_2-Ar), 6.15 (s, 4H, Cp*H*), 6.80−7.60 (m, 10H, −Ar*H*). ^{13}C NMR ($CDCl_3$): δ 27.1 [−*C*H$_2$−], 28.7 [−*C*H$_2$−], 32.1 [−*C*H$_2$−], 36.5 [C-*C*H$_2$-Ar], 116.9 [−*C*H Cp], 126.3 [C$_q$], 126.5 [C$_q$], 128.3 [*C*H Ar], 128.4 [*C*H Ar], 128.5 [*C*H Ar], 133.8 [C$_q$]. Anal. calcd for $C_{34}H_{38}Cl_2Zr$ (608.80): C, 67.1; H, 6.3; Cl, 11.6. Found: C, 67.4; H, 6.1; Cl, 11.2.

Bis[η^5-(2-benzyl-4,5,6,7,8-hexahydroazulenyl)]titanium Dichloride (C_7Bn-Ti). A solution of chlorotrimethylsilane (30 mmol) in THF (10 mL) was added dropwise to the lithium salt (**3**) (10 mmol), dissolved in anhyd THF (30 mL). The resulting solution was stirred 6 h at room temperature, then cooled to 0 °C, and a saturated aqueous solution of NH_4Cl was slowly added until there was separation of two phases. After separation, the aqueous solution was washed three times with diethyl ether. The collected organic fractions were dried over anhyd $MgSO_4$, filtered, and then the solvent was removed at the rotary evaporator. The trimethylsilyl derivative (**4**) was transferred into a Schlenk flask, degassed, protected from light, and then dissolved in CH_2Cl_2 (about 30 mL). A solution of $TiCl_4$ (4.8 mmol) in CH_2Cl_2 (5 mL) was added dropwise, and the reaction mixture was stirred overnight. The solvent was removed under vacuum, and the residue was washed with petroleum ether, filtered, and dried under reduced pressure to give a red-brown microcrystalline solid. Yield 75%. ^{1}H NMR ($CDCl_3$): δ 1.05−2.2 (m, 20H, −CH_2−), 2.80 (s, 4H, Cp-CH_2-Ar), 6.60−7.60 (m, 24H). Anal. calcd for $C_{34}H_{38}Cl_2Ti$ (565.43): C, 72.2; H, 6.8; Cl, 12.5. Found: C, 72.0; H, 6.3; Cl, 12.1.

Crystal Structure Determination of C_7Bn-Zr. The crystal data of **C_7Bn-Zr** were collected using a Nonius Kappa CCD diffractometer with graphite-monochromated Mo Kα radiation. Before analysis, the crystals were protected by moisture and air with Nujol previously dehydrated with K and degassed. The data sets were integrated with the Denzo-SMN package[24] and corrected for Lorentz, polarization, and absorption (SORTAV[25]) effects. The structure was solved by direct methods (SIR97)[26] and refined using full-matrix least-squares with all nonhydrogen atoms anisotropic and hydrogens included on calculated positions, riding on their carrier atoms. All calculations were performed using SHELXL-97[27] and PARST[28] implemented in the WINGX[29] system of programs. Crystal Data: $C_{34}H_{38}Cl_2Zr$; monoclinic, space group $C2/c$, a = 18.901(2), b = 6.512(1), c = 23.870(3) Å, β = 94.540(4)°, V = 2909.0(7) Å^3, $Z = 4$, $Dc = 1.380$ g cm^{-3}. Intensity data collected with $\theta \leq 24°$; 2303 independent reflections measured, 1021 reflections observed [$I > 2\sigma(I)$]. Final $R = 0.036$ (observed reflections), and $R_w = 0.096$ (all reflections). Selected interatomic distances and angles are given in Table 1.

Propene Polymerizations. Manipulations of air- and/or moisture-sensitive materials were carried out under inert atmosphere using a dual vacuum/nitrogen line and standard Schlenk techniques, or in a drybox under nitrogen atmosphere (<10 ppm oxygen, <20 ppm water). To prevent possible

photodecomposition, Ti complexes solutions were carefully protected from light during the preparative steps of the polymerization experiments. Toluene was dried by distillation from sodium under nitrogen atmosphere. Methylaluminoxane (MAO) (Witco, 10 wt. % solution in toluene) was used after drying in a vacuum to remove the solvent and unreacted trimethylaluminum (TMA), and then was stored under nitrogen. Nitrogen and propene were purified by passage through columns of BASF RS-11 (Fluka) and Linde 4 Å molecular sieves.

In a typical polymerization reaction, a 250-mL Büchi autoclave equipped with a mechanical stirrer was charged under nitrogen with a solution of 7.5 mmol of dry methylaluminoxane (MAO) in 100 mL of anhyd toluene. A 25-mL injector was charged with 10 mL of a solution of 10 μmol of catalyst and 2.5 mmol of MAO in toluene (total MAO/Mt ratio = 1000). After thermal equilibration of the reactor system at the proper temperature, propene was continuously added until saturation. The injector with the metallocene solution was pressurized to 3 atm with nitrogen, and the solution was injected into the reactor. The solution was stirred for 30 min. The reaction was terminated by addition of a small amount of ethanol, and the polymer was precipitated upon pouring the whole reaction mixture into ethanol (600 mL) to which concentrated hydrochloric acid (5 mL) had been added. The polymer was collected by filtration and dried under vacuum at 70 °C.

Nuclear Magnetic Resonance (NMR). ^{13}C NMR spectra of the polymers were recorded in $C_2D_2Cl_4$ at 103 °C on a Bruker AM-400 spectrometer operating at 100.58 MHz (internal chemical shift reference: 1% hexamethyldisiloxane). Conditions: 10 mm probe; 90° pulse angle; 64 K data points; acquisition time 5.56 s; relaxation delay 20 s; 3−4 K transients. Proton broad-band decoupling was achieved with a 1D sequence using bi_waltz16_32 power-gated decoupling.

Size Exclusion Chromatography (SEC). Molecular mass distributions were determined by using a GPCV2000 size-exclusion chromatography (SEC) system from Waters, equipped with a differential refractometer. The column set was composed of three mixed TSK−Gel GMH_{XL}-XT columns from Tosohaas (mobile phase = *o*-dichlorobenzene; temperature = 145 °C; flow rate = 0.8 mL/min; injection volume = 300 mL).

Thermal Analysis. Differential scanning calorimetry (DSC) scans were carried out on a Perkin-Elmer Pyris 1 instrument equipped with a liquid subambient device under nitrogen atmosphere. Typically, ca 5 mg of polymer were heated to 200 °C and held at this temperature for 3 min to cancel previous thermal history. Then, the samples were cooled to 20 °C at 10 °C/min rate and held at room temperature for 5 min. The aged samples were prepared by cooling the polymers from 200 to 20 °C under controlled conditions (10 °C/min) and annealing them for long times (5−30 days) at room temperature. Finally, the samples were heated with a scan rate of 20 °C/min to 200 °C, determining the melting transition and the enthalpy of fusion.

X-ray Analysis. The wide-angle X-ray diffraction (WAXD) data were obtained at 20 °C using a Siemens D-500 diffractometer equipped with a Siemens FK 60−10 2000 W tube (Cu Kα radiation, λ = 0.154 nm); operating voltage = 40 kV; current = 40 mA. The data were collected from 5 to 30 2θ° at 0.02 2θ° intervals.

Acknowledgment. We warmly thank Mr. G. Zannoni who has carefully and expertly performed all the NMR spectra and Mr. M. Canetti for his helpful contribution to X-ray analyses.

Supporting Information Available: X-ray crystallographic data in CIF format. This material is available free of charge via the Internet at http://pubs.acs.org.

References and Notes

(1) For example (review): (a) Jordan, R. F. *Adv. Organomet. Chem.* **1991**, *32*, 325−387. (b) Möhring, P. C.; Coville, N. J. *J. Organomet. Chem.* **1994**, *479*, 1−29. (c) Brintzinger, H.-H.; Fischer, D.; Mülhaupt, R.; Rieger, B.; Waymouth, R. M. *Angew. Chem., Int. Ed. Engl.* **1995**, *34*, 1143−1170. (d) Bochmann, M. *J. Chem. Soc., Dalton Trans.* **1996**, 225−270. (e) Kaminsky, W.; Arndt, M. *Adv. Polym. Sci.* **1997**, *127*, 143−187. (f) Resconi, L.; Cavallo, L.; Fait, A.; Piemontesi, F. *Chem. Rev.* **2000**, *100*, 1253−1346. (g) Kaminsky, W. *J. Polym. Sci., Part A: Polym. Chem.* **2004**, *42*, 3911−3921.

(2) (a) Natta, G.; Mazzanti, G.; Crespi, G.; Moraglio, G. *Chim. Ind. (Milan)* **1957**, *39*, 275−283. (b) Natta, G. *J. Polym. Sci.* **1959**, *34*, 531−549.

(3) (a) Collette, J. W.; Tullock, C. W.; MacDonald, R. N.; Buck, W. H.; Su, A. C. L.; Harrel, J. R.; Mülhaupt, R.; Anderson, B. C. *Macromolecules* **1989**, *22*, 3851−3858. (b) Collette, J. W.; Ovenall, D. W.; Buck, W. H.; Ferguson, R. C. *Macromolecules* **1989**, *22*, 3858−3866.

(4) (a) Mallin, D. T.; Rausch, M. D.; Lin, Y. G.; Dong, S.; Chien, J. C. W. *J. Am. Chem. Soc.* **1990**, *112*, 2030−2031. (b) Chien, J. C. W.; Tsai, W.-M.; Rausch, M. D. *J. Am. Chem. Soc.* **1991**, *113*, 8570−8571. (c) Babu, G. N.; Newmark, R. A.; Cheng, H. N.; Llinas, G. H.; Chien, J. *Macromolecules* **1992**, *25*, 7400−7402. (d) Gauthier, W. J.; Corrigan, J. F.; Taylor, N. J.; Collins, S. *Macromolecules* **1995**, *28*, 3771−3778. (e) Gauthier, W. J.; Collins, S. *Macromolecules* **1995**, *28*, 3779−3786.

(5) (a) Coates, G.; Waymouth, R. M. *Science* **1995**, *267*, 217−219. (b) Hauptman, E.; Waymouth, R. M.; Ziller J. W. *J. Am. Chem. Soc.* **1995**, *117*, 11586−11587.

(6) (a) Lin, S.; Waymouth, R. M. *Acc. Chem. Res.* **2002**, *135*, 765−773 and refs. therein. (b) Reybuck, S. E.; Meyer, A.; Waymouth, R. M. *Macromolecules* **2002**, *35*, 637−643. (c) Dankova, M.; Kravchenko, R. L.; Cole, A. P.; Waymouth, R. M. *Macromolecules* **2002**, *35*, 2882−2891. (d) Gómez, F. J.; Waymouth, R. M. *Macromolecules* **2002**, *35*, 3358−3368. (e) Wilmes, G. M.; Lin, S.; Waymouth, R. M. *Macromolecules* **2002**, *35*, 5382−5387. (f) Wilmes, G. M.; Polse, J. L.; Waymouth, R. M. *Macromolecules* **2002**, *35*, 6766−6772. (g) Fan, W.; Waymouth, R. M. *Macromolecules* **2003**, *36*, 3010−3014. (h) Dankova, M.; Waymouth, R. M. *Macromolecules* **2003**, *36*, 3815−3820. (i) Wiyatno, W.; Chen, Z.-R.; Liu, Y.; Waymouth, R. M.; Krukonis, V.; Brennan, K. *Macromolecules* **2004**, *37*, 701−708. (j) Reybuck, S. E.; Waymouth, R. M. *Macromolecules* **2004**, *37*, 2342−2347. (k) Wilmes, G. M.; France, M. B.; Lynch, S. R.; Waymouth, R. M. *Organometallics* **2004**, *23*, 2405−2411.

(7) (a) Schneider, N.; Schaper, F.; Schmidt, K.; Kirsten, R.; Geyer, A.; Brintzinger, H.-H. *Organometallics* **2000**, *19*, 3597−3604. (b) Busico, V.; Cipullo, R.; Kretschmer, W. P.; Talarico, G.; Vacatello, M.; Castelli, V. V. A. *Angew. Chem., Int. Ed. Engl.* **2002**, *41*, 505−508. (c) Busico, V.; Cipullo, R.; Kretschmer, W. P.; Talarico, G.; Vacatello, M.; Castelli, V. V. A. *Macromolecules* **2001**, *34*, 8412−8415. (d) Busico, V.; Cipullo, R.; Kretschmer, W. P.; Talarico, G.; Vacatello, M.; Castelli, V. V. A. *Macromol. Symp.* **2002**, *189*, 127−141.

(8) Wilmes, G. M.; France, M. B.; Lynch, S. R.; Waymouth, R. M. *Organometallics* **2004**, *23*, 2405−2411.

(9) (a) Erker, G.; Nolte, R.; Schlund, R.; Benn, R.; Grodney, H.; Mynott, R. *J. Organomet. Chem.* **1989**, *364*, 119−132. (b) Erker, G.; Nolte, R.; Aul, R.; Wilker, S.; Krüger, C.; Noe, R. *J. Am. Chem. Soc.* **1991**, *113*, 7594−7602. (c) Erker, G.; Temme, B. *J. Am. Chem. Soc.* **1992**, *114*, 4004−4006. (d) Erker, G.; Aulbach, M.; Knickmeier, M.; Wingbermühle, D.; Krüger, C.; Nolte, M.; Werner, S. *J. Am. Chem. Soc.* **1993**, *115*, 4590−4601. (e) Krüger, C.; Lutz, F.; Nolte, M.; Erker, G.; Aulbach, M. *J. Organomet. Chem.* **1993**, *452*, 79−86. (f) Knüppel, S.; Fauré, J. L.; Erker, G.; Kehr, G.; Nissinen, M.; Fröhlich, R. *Organometallics* **2000**, *19*, 1262−1268. (g) Dreier, T.; Unger, G.; Erker, G.; Wibbeling, B.; Fröhlich, R. *J. Organomet. Chem.* **2001**, *622*, 143−148. (h) Dreier, T.; Fröhlich, R.; Erker, G. *J. Organomet. Chem.* **2001**, *621*, 197−206. (i) Dreier, T.; Bergander, K.; Wegelius, E.; Fröhlich, R.; Erker, G. *Organometallics* **2001**, *20*, 5067−5075.

(10) (a) Grimmer, N. E.; Coville, N. J.; de Koning, C. B.; Smith, J. M.; Cook, L. M. *J. Organomet. Chem.* **2000**, *616*, 112−127. (b) Bravakis, A. M.; Bailey, L. E.; Pigeon, M.; Collins, S. *Macromolecules* **1998**, *31*, 1000−1009.

(11) (a) Maciejewski Petoff, J. L.; Myers, C. L.; Waymouth, R. M. *Macromolecules* **1999**, *32*, 7984−7989. (b) Wilmes, G. M.; Polse, J. L.; Waymouth, R. M. *Macromolecules* **2002**, *35*, 6766−6772. (c) Rodriguez-Delgado, A.; Hannant, M. D.; Lancaster, S. J.; Bochmann, M. *Macromol. Chem. Phys.* **2004**, *205*, 334−346. (d) Song, F.; Hannant, M. D.; Cannon, R. D.;

Bochmann, M. *Macromol. Symp.* **2004**, *213*, 173−186. (e) Fujita, M.; Seki, Y.; Miyatake, T. *Macromolecules* **2004**, *37*, 9676−9680.
(12) (a) Schmidt, R.; Alt, H. G. *J. Organomet. Chem*. **2001**, *621*, 304−309. (b) Schmidt, R.; Deppner, M.; Alt, H. G. *J. Mol. Catal. A: Chem.* **2001**, *172*, 43−65.
(13) Polo, E.; Losio, S.; Forlini, F.; Locatelli, P.; Provasoli, A.; Sacchi, M. C. *Macromol. Chem. Phys.* **2002**, *203*, 1859−1865.
(14) (a) Polo, E.; Losio, S.; Forlini, F.; Locatelli, P.; Sacchi, M. C. *Macromol. Symp.* **2004**, *213*, 89−99. (b) Polo, E., Losio, S.; Zecchi, G.; Bertini, F.; Sacchi, M. C. *Macromol. Rapid. Comm.* **2004**, *25*, 1845−1850.
(15) Polo, E.; Barbieri, A.; Traverso O. *New J. Chem.* **2004**, *28*, 652−656.
(16) Polo, E.; Barbieri, A.; Traverso O. *Eur. J. Inorg. Chem*. **2003**, *9*, 324−330.
(17) Polo, E.; Bellabarba, R. M.; Prini, G.; Traverso O.; Green, M. L. H. *J. Organomet. Chem.* **1999**, *577*, 211−218.
(18) Burdett, M. N.; Johnson, C. K. *ORTEP III*, Report ORNL-6895; Oak Ridge National Laboratory: Oak Ridge, TN, 1996.
(19) (a) Gallucci, J. C.; Gautheron, B.; Gugelchuk, M.; Meunier, P.; Paquette, L. A. *Organometallics* **1987**, *6*, 15−19. (b) Paquette, L. A.; Moriarty, K. J.; McKinney, J. A.; Rogers, R. D. *Organometallics* **1989**, *8*, 1707−1713. (c) Herrmann, W. A.; Anwander, R.; Riepl, H.; Scherer, W.; Whitaker, C. R. *Organometallics* **1993**, *12*, 4342−4349. (d) Halterman, R. L.; Chen, Z. *J. Organomet. Chem*. **1995**, *503*, 53−57.
(20) (a) Hauptman, E.; Waymouth, R. M. *J. Am. Chem. Soc*. **1995**, *117*, 11586−11587. (b) Bradley, C. A.; Flores-Torres, S.; Lobkovsky, E.; Abruna, H. D.; Chirik, P. J. *Organometallics* **2004**, *23*, 5332−5346.
(21) Mansel, S.; Pérez, E.; Benavente, R. J.; Pereña, M.; Bello, A.; Roll, W.; Kirsten, R.; Beck, S.; Brintzinger, H.-H. *Macromol. Chem. Phys.* **1999**, *200*, 1292−1297.
(22) See, e.g.: Hu, Y.; Kreychi, M. T.; Shah, C. D.; Myers, C. L.; Waymouth, R. M. *Macromolecules* **1998**, *31*, 6908−6916.
(23) Manzer, L. E. *Inorg. Synth.* **1982**, *21*, 135−137.
(24) Otwinowski, Z.; Minor, W. In *Methods in Enzymology*; Carter, C. W., Sweet, R. M., Eds.; Academic Press: London, 1997; Vol. 276, Part A, pp 307−326.
(25) Blessing, R. H. *Acta Crystallogr., Sect A* **1995**, *51*, 33−38.
(26) Altomare, A.; Burla, M. C.; Camalli, M.; Cascarano, G. L.; Giacovazzo, C.; Guagliardi, A.; Moliterni, A. G. G.; Polidori, G.; Spagna, R. *J. Appl. Crystallogr*. **1999**, *32*, 115−119.
(27) Sheldrick, G. M. *SHELX-97*, Program for Crystal Structure Refinement; University of Gottingen: Germany, 1997.
(28) Nardelli, M. *J. Appl. Crystallogr.* **1995**, *28*, 659−659.
(29) Farrugia, L. J. *J. Appl. Crystallogr*. **1999**, *32*, 837−838.

MA050599T